RELATIVISTIC HEAVY ION EXCITATION OF GIANT RESONANCES

C.A. BERTULANI
NSCL, Michigan State University,
East Lansing, MI 48824-1321, USA

Giant resonances and giant resonances built on other giant resonances in nuclei are observed with very large cross sections in relativistic heavy ion collisions. A theoretical effort is underway to understand the reaction mechanism which leads to this process, as well as a better understanding of the microscopic properties of multiphonon states, e.g., their strength, energy centroids, widths and anharmonicities.

1 Giant Resonances

1.1 Single giant resonances

Giant resonances in nuclei were first observed in 1937 by Bothe and Gentner [1] who obtained an unexpectedly large absorption of 17.6 MeV photons (from the ^{7}Li(p,γ) reaction) in some targets. These observations were later confirmed by Baldwin and Klaiber (1947) with photons from a betatron. In 1948, Goldhaber and Teller [2] interpreted these resonances (called isovector giant dipole resonances (IVGDP)) with a hydrodynamical model in which rigid proton and neutron fluids vibrate against each other, the restoring force resulting from the surface energy. Steinwendel and Jensen [3] later developed the model, considering compressible neutron and proton fluids vibrating in opposite phase in a common fixed sphere, the restoring force resulting from the volume symmetry energy. The standard microscopic basis for the description of giant resonances is the random phase approximation (RPA) in which giant resonances appear as coherent superpositions of one-particle one-hole ($1p1h$) excitations in closed shell nuclei or two quasiparticle excitations in open shell nuclei (for a review of these techniques, see, for example, ref. [4]). The isoscalar quadrupole resonances were discovered in inelastic electron scattering by Pitthan and Walcher (1971) and in proton scattering by Lewis and Bertrand (1972). Giant monopole resonances were found later and their properties are closely related to the compression modulus of nuclear matter. Following these, other resonances of higher multipolarities and giant magnetic resonances were investigated. Typical probes for giant resonance studies are (a) γ's and electrons for the excitation of IVGDR, (b) α-particles and electrons for the excitation of isoscalar giant monopole resonance (ISGMR) and giant quadrupole resonance (ISGQR), and (c) (p, n), or (^{3}He, t), for Gamow-Teller resonances, respectively.

1.2 Multiphonon resonances

Inelastic scattering studies with heavy ion beams have opened new possibilities in the field (for a review of the recent developments, see ref. [5]). A striking feature was observed when either the beam energy was increased, or heavier projectiles were used, or both [6]. This is displayed in figure 1, where the excitation of the GDR in ^{208}Pb was observed in the inelastic scattering of ^{17}O at

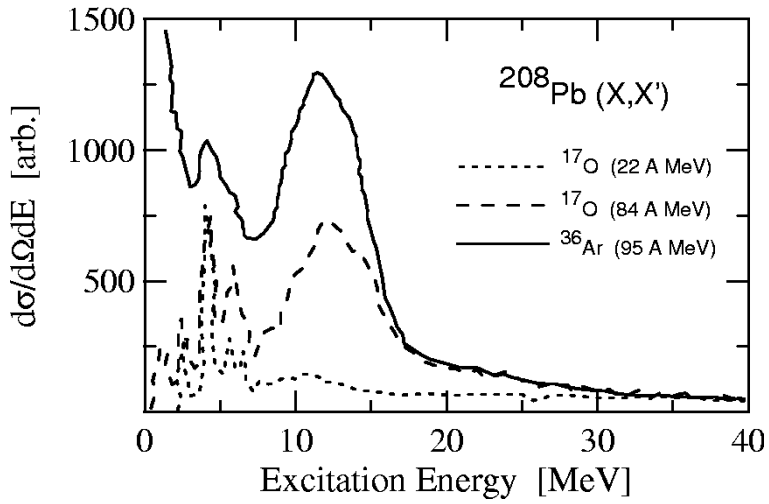

Figure 1: Experimental cross sections in arbitrary units for the excitation of ^{208}Pb targets by ^{17}O (22.A MeV and 84.A MeV) and by ^{36}Ar (95.A MeV), as a function of the excitation energy.

22 MeV/nucleon and 84 MeV/nucleon, respectively, and ^{36}Ar at 95 MeV/nucleon[7,8]. What one clearly sees is that the 'bump' corresponding to the GDR at 13.5 MeV is appreciably enhanced. This feature is solely due to one agent: the electromagnetic interaction between the nuclei. This interaction is more effective at higher energies, and for increasing charge of the projectile. In ref. [9] it was shown that the excitation probabilities of the GDR in heavy ion collisions approach unity at grazing impact parameters. It was also obtained that, if the DGDR (double GDR), or GDR^2 (i.e., a GDR excited on a GDR state), exists then their excitation cross sections in heavy ion collisions at relativistic energies are of the order of hundreds of millibarns. The calculation was based on the semiclassical approach, appropriate for heavy ion scattering at high incident energies, and the harmonic oscillator model for the giant resonances. The semiclassical model treats the relative motion between the nuclei classically while quantum mechanics is used for the internal degrees of freedom. In the harmonic picture for the internal degrees of freedom the GDR is the first excited state in a harmonic well, the DGDR is the second state, and so on. In ref. [10] it was shown that the excitation probabilities and cross sections are directly proportional to the photonuclear cross sections for a given electric (E) and magnetic (M) multipolarity. For an impact parameter b, excitation energy E , and a multipolarity $\pi\lambda$ (π = E or M, λ = 1, 2, 3, $\cdots$) the excitation probabilities are given by

$$P_{\pi\lambda}(E,b) = \frac{1}{E} N_{\pi\lambda}(E,b)\sigma_\gamma^{\pi\lambda}(E) \qquad (1)$$

where $\sigma_\gamma^{\pi\lambda}(E)$ is the photonuclear cross sections for the photon E and multipolarity $\pi\lambda$. The total photonuclear cross section is $\sigma_\gamma(E) = \sum_{\pi\lambda} \sigma_\gamma^{\pi\lambda}(E)$. In the semiclassical approach, the *equivalent photon numbers* $N_{\pi\lambda}(E,b)$ are given analytically [10]. A quantum mechanical derivation of the excitation amplitudes in relativistic Coulomb excitation shows that equation (1) can also be obtained by using the saddle-point approximation in the DWBA integrals [11]. The total Coulomb excitation cross sections are then obtained by an integration of equation (1) over the impact parameter b, including a factor, $T(b)$, which accounts for the strong absorption at small impact parameters: $\sigma_{\pi\lambda}(E) = 2\pi \int db\ b\ T(b) P_{\pi\lambda}(E,b)$. The total number of equivalent photons $n_{\pi\lambda}(E) = 2\pi \int db\ b\ N_{\pi\lambda}(E,b)$ is given in [10,11]. The cross section for the excitation of a giant resonance is obtained from these expressions, by using the experimental photonuclear absorption cross section for $\sigma_\gamma^{\pi\lambda}(E)$ in equation (1). One problem with this procedure is that the experimental photonuclear cross section includes all multipolarities with the same

weight: $\sigma_\gamma^{exp}(E) = \sum_{\pi\lambda} \sigma_\gamma^{\pi\lambda}(E)$, while the calculation based on equation (1) needs the isolation of $\sigma_\gamma^{\pi\lambda}(E)$. This can only be done marginally, except in some exclusive measurements. Generally, one finds in the literature the (γ, n), (γ, 2n), and (γ, 3n) cross sections, which include the contribution of all multipolarities in the giant resonance energy region. A separation of the different multipolarities can be obtained roughly by use of sum rules, or some theoretical model for the nuclear response to a photoexcitation. Assuming that one has $\sigma_\gamma^{\pi\lambda}(E)$ somehow (either from experiments, or from theory), a simple harmonic model based on the Axel–Brink hypotheses can be formulated to obtain the probability to access a multiphonon state of order n. In the harmonic oscillator model the inclusion of the coupling between all multiphonon states can be performed analytically [9]. One of the basic changes is that the excitation probabilities calculated to first-order, $P_{\pi\lambda}^{1st}(E,b)$, are modified to include the flux of probability to the other states. That is, for the first harmonic state,

$$P_{\pi\lambda}(E,b) = P_{\pi\lambda}^{1st}(E,b) \exp\left\{-P_{\pi\lambda}^{1st}(b)\right\}, \tag{2}$$

where $P_{\pi\lambda}^{1st}(b)$ is the integral of $P_{\pi\lambda}^{1st}(E,b)$ over the excitation energy E. In general, the probability to reach a multiphonon state with the energy $E^{(n)}$ from the ground state, with energy $E^{(0)}$, is obtained by an integral over all intermediate energies

$$\begin{aligned} P_{\pi^*\lambda^*}^{(n)}(E^{(n)},b) &= \frac{1}{n!} \exp\left\{-P_{\pi\lambda}^{1st}(b)\right\} \int dE^{(n-1)} dE^{(n-2)} \cdots dE^{(1)} \\ &\times \; P_{\pi\lambda}^{1st}(E^{(n)} - E^{(n-1)}, b) P_{\pi\lambda}^{1st}(E^{(n-1)} - E^{(n-2)}, b) \cdots P_{\pi\lambda}^{1st}(E^{(1)} - E^{(0)}, b). \end{aligned} \tag{3}$$

The character and spin assignment of the multipolarity λ^* depends on how the intermediate states couple with the electromagnetic transition operators. For example, in the case of the DGDR (GDR^2), assuming a 0^+ ground state and excluding isospin impurities, the final state has either spin and parity 0^+ or 2^+, respectively. A simpler reaction model than the one above can be obtained by assuming that all states can be approximated by a single isolated state. For example, we can assume that the photoabsorption cross sections in the range of the GDR is due to a single state with energy equal to the centroid energy of the GDR exhausting the whole excitation strength. Then the multiphonon states are sharp and equidistant. Eq. (3) becomes

$$P_{\pi^*\lambda^*}^{(n)}(b) = \frac{1}{n!} [P_{\pi\lambda}^{1st}(b)]^n \exp\left\{-P_{\pi\lambda}^{1st}(b)\right\}. \tag{4}$$

The above relation was used to calculate the cross sections for the excitation of the GDR, GDR^2, GDR^3, ISGQR and IVGQR in ^{136}Xe, respectively, for collisions with Pb nuclei as a function of the bombarding energy, as shown in figure 2. Each resonance is considered to be a single state exhausting 100% of the respective sum rule. Also shown in the figure is the geometrical cross section, (GC), $\sigma \sim \pi(A_P^{1/3} + A_T^{1/3})^2$ fm^2 . The cross sections for the excitation of the GDR^2 is large, of the order of hundreds of mb. Much of the interest in looking for multiphonon resonances relies on the possibility of finding exotic particle decay of these states. For example, in ref. [15] a hydrodynamical model was used to predict the proton and neutron dynamical densities in a multiphonon state of a nucleus. Large proton and neutron excesses at the surface are present in a multiphonon state. Thus, the emission of exotic clusters from the decay of these states are a natural possibility. A more classical point of view is that the Lorentz contracted Coulomb field in a peripheral relativistic heavy ion collision acts as a hammer on the protons of the nuclei [10]. This (collective) motion of the protons seems only to be probed in relativistic Coulomb excitation.

Despite all the advantages of relativistic Coulomb excitation, the DGDR was first found in pion scattering at the Los Alamos Pion Facility [12]. In pion scattering off nuclei the DGDR can be described as a two-step mechanism induced by the pion-nucleus interaction. Only about

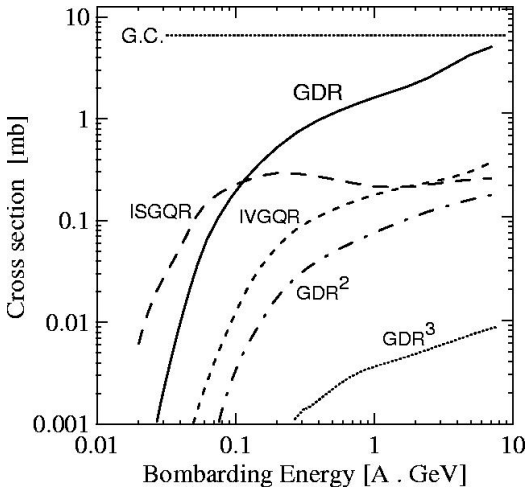

Figure 2: Theoretical cross sections for the excitation of the GDR, ISGQR, IVGQR, GDR^2 and the GDR^3 , in the reaction ^{208}Pb + ^{208}Pb, as a function of the bombarding energy.

five years later, the first Coulomb excitation experiments for the excitation of the DGDR were performed at the GSI facility in Darmstadt/Germany [13,14]. One of these experiments observed the neutron decay channels of giant resonances excited by relativistic projectiles. The excitation spectrum of relativistic ^{136}Xe projectiles incident on Pb were compared with the spectrum obtained in C targets. A comparison of the two spectra immediately proved that the nuclear contribution to the excitation is very small. Another experiment [14] dealt with the photon decay of the double giant resonance. The advantages of relativistic Coulomb excitation of heavy ions over other probes (pions, nuclear excitation, etc.) was clearly demonstrated in several other GSI experiments [13,14,16,17].

2 Energy, width and strength of the DGDR

Experimentally [18], it was found that the energy of the DGDR agrees with the harmonic prediction, i.e., that its energy should be twice the energy of the GDR, although small departures from this prediction were seen, especially in pion and nuclear excitation experiments. The width of the DGDR seems to be $\sqrt{2}$ times that of the GDR, although a value equal to 2 is not ruled out completely. An unexpected result was obtained for the ratio between the measured cross sections and the calculated ones. This seems to be strongly dependent on the experimental probe. The largest values of σ_{exp}/σ_{th} come from pion experiments, yielding up to a value of 5 for it. In Coulomb excitation experiments this ratio was initially [13,14] of the order of 2.

2.1 Width of the DGDR

In a microscopic approach, the GDR is described as a coherent superposition of one-particle one-hole states. One of the many such states is pushed up by the residual interaction to the experimentally observed position of the GDR. This state carries practically all of the E1 strength. This situation is simply realized in a model with a separable residual interaction. We write the GDR state as (one phonon with angular momentum $1M$) $|1,1M>= A^{\dagger}_{1M}|0>$, where $A^{\dagger}_{1M}$ is a proper superposition of particle-hole creation operators. Applying the quasi-boson approximation we can use the boson commutation relations and construct the multiphonon states (N-phonon states). An N-phonon state will be a coherent superposition of N-particle N-hole states. The width of the GDR is essentially due to the spreading width, i.e., to the coupling

to more complicated quasi-bound configurations. The escape width only plays a minor role. Let us take a simple model for the strength function[19]. A state $|a>$ (i.e., a GDR state) is coupled by some mechanism to more complicated states $|\alpha>$. For simplicity we assume a constant coupling matrix element $V_{a\alpha} =< a|V|\alpha >=< \alpha|V|a >= v$. With an equal spacing of D of the levels $|\alpha>$ one obtains a width $\Gamma = 2\pi v^2/D$ for the state $|a>$. We assume the same mechanism to be responsible for the width of the N-phonon state: one of the N-independent phonons decays into the more complicated states $|\alpha>$ while the other (N - 1)-phonons remain spectators. We write the coupling interaction in terms of creation (destruction) operators $c^\dagger_\alpha$ (c_α) of the complicated states $|\alpha>$ as

$$V = v(A^\dagger_{1M} c_\alpha + A_{1M} c^\dagger_\alpha). \tag{5}$$

For the coupling matrix elements v_N, which connects an N-phonon state $|N>$ to the state $|N-1, \alpha>$ (N-1 spectator phonons) one obtains

$$vN =< N-1, \alpha|V|N >= v < N-1|A_{1M}|N >= v\sqrt{N}, \tag{6}$$

i.e., one obtains for the width Γ_N of the N-phonon state

$$\Gamma_N = 2\pi N \frac{v^2}{D} = N\Gamma \ . \tag{7}$$

Thus, the factor N in (7) arises naturally from the bosonic character of the collective states. For the DGDR this would mean $\Gamma_2 = 2\Gamma_1$. The data points seem to favor a lower multiplicative factor.

We can also give a qualitative explanation for a smaller Γ_2/Γ_1 value. First we note that the value $\Gamma_2/\Gamma_1 = 2$ can also be obtained from a folding procedure, as given in equation (3). If the sequential excitations are described by Breit-Wigner (BW) functions $P_{\pi\lambda}(E)$ with the centroid $\mathcal{E}$ and the width Γ, the convolution (3) yields a BW shape with the centroid at $2\mathcal{E}$ for the DGDR and the total width of $2\Gamma_1$. However, if one uses Gaussian functions (instead of BW) for the shape of one-phonon states, it is easy to show that one also obtains a Gaussian for the N-phonon shape, but with the width given by $\sqrt{N}\Gamma_1$. The latter assumption seems inconsistent since the experimentalists use BW fits for the shape of giant resonances, which are in good agreement with the experimental data. However, one can easily understand that the result $\sqrt{N}\Gamma_1$ is not restricted to a Gaussian fit. For an arbitrary sequence of two excitation processes we have $< E >=< E_1 + E_2 >$ and $< E^2 >=< (E_1 + E_2)^2 >$; for uncorrelated steps it results in the addition in quadrature $(\Delta E)^2 = (\Delta E_1)^2 + (\Delta E_2)^2$. Identifying these fluctuations with the widths up to a common factor, we obtain for identical phonons $\Gamma_2 = \sqrt{2}\Gamma_1$. The same conclusion will be valid for any distribution function which, as the Gaussian one, has a finite second moment, in contrast to the BW or Lorentzian ones with second moment diverging. We may conclude that, in physical terms, the difference between $\Gamma_2/\Gamma_1 = 2$ and $\Gamma_2/\Gamma_1 = \sqrt{2}$ is due to the different treatment of the wings of the distribution functions which reflect small admixtures of remote states.

2.2 Strength of the DGDR

Microscopically, the harmonic picture is accomplished within the RPA approximation. The excited states of the nucleus are described as superpositions of particle-hole configurations with respect to the ground state. The multiphonon resonances are built using products of the 1^- resonance states, yielding 0^+ and 2^+ double phonon states. The interaction with the projectile is described in terms of a linear combination of particle-hole operators weighted by the time-dependent field for a given multipolarity of the interaction. Since the time-dependent Coulomb field of a nucleus does not carry monopole multipolarity, the DGDR states can be reached via

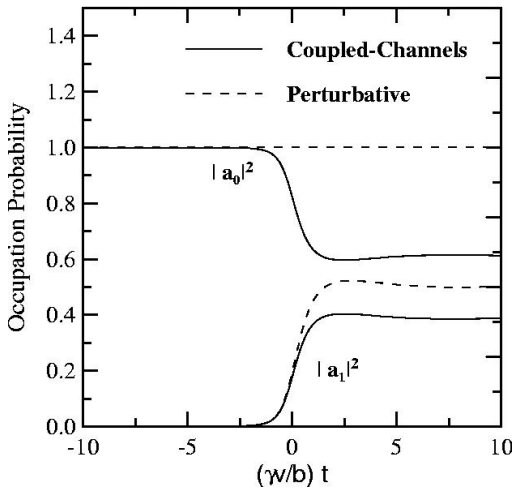

Figure 3: Occupation probability of the ground state, $|a_0|^2$, and of the GDR, $|a_1|^2$, for the reaction ^{208}Pb + ^{208}Pb at 640.A MeV, as a function of the reaction time. The reaction time is given in terms of the adimensional quantity $\gamma vt/b$, with b equal to the impact parameter in the collision. The broken curves are the predictions of perturbation theory, while the full curves are the predictions of coupled–channels calculations.

two-step E1 transitions and direct E2 transitions (for a 0^+ ground state). Early calculations failed to explain the experimental data.

There seems to be two possible reasons for $\sigma_{exp}/\sigma_{th} \neq 1$; (a) either the Coulomb excitation mechanism is not well described, or (b) the response of the nucleus to two-phonon excitations is not well known.

Many authors studied the effects of the excitation mechanism of the DGDR. In ref. [20] the cross sections were calculated using second-order perturbation theory. It was found that the theoretical values were smaller than the experimental ones by a factor of $1.3 - 2$. However, it was suggested [21] that second-order perturbation theory is not adequate for relativistic Coulomb excitation of giant resonances with heavy ions and that it is necessary to perform a coupled channels calculation. We can see this more clearly in figure 3, taken from [22], where a coupled-channels study of multiphonon excitation by the nuclear and Coulomb interactions in relativistic heavy ion collisions was performed. The figure shows the probability amplitude to excite the GDR in ^{208}Pb, $|a_1|^2$, and the occupation probability of the ground state, $|a_0|^2$, for a grazing collision of ^{208}Pb + ^{208}Pb at 640 MeV/nucleon. The broken curves are the predictions of the first-order perturbation theory. We see that the asymptotic excitation probability of the GDR is quite large (40%). In first-order perturbation theory the occupation probability of the ground state is kept constant, equal to unity. Obviously, one greatly violates the unitarity condition in this case. An appropriate coupled-channels calculation (full curves) shows that the ground-state occupation probability has to decrease to meet the unitarity requirements, while the excitation probability of the GDR is also reduced slightly for the same reason. In ref. [22] it was shown that a good coupled-channels calculation does not need to account for the exact coupling equations in all channels. The strongest coupling, responsible for the effect observed in figure 3 is the coupling between the ground state and the GDR states. This has to be treated exactly within a coupled-channels calculation. The coupling between the GDR and the other states (including the DGDR, IVGQR, ISGQR, etc.) can be treated perturbatively.

The results of [22] showed appreciable dependence of the excitation cross sections of the DGDR on the width of both the GDR and the DGDR for ^{208}Pb + ^{208}Pb at 640 MeV/nucleon. It was also shown that the most favorable energies for the measurement of the DGDR corresponds to the SIS energies at the GSI/Darmstadt facility.

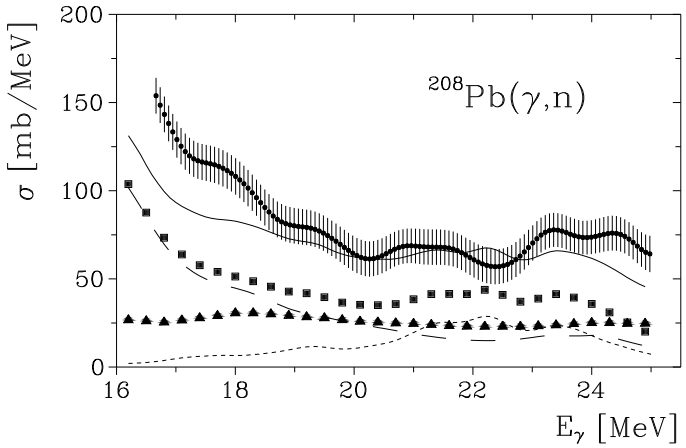

Figure 4: Photoneutron cross section for ^{208}Pb. Experimental data (dots with experimental errors) are from ref. [28]. The long-broken curve is the high-energy tail of the GDR, the short-broken curve is the IVGQR and the curve with squares is their sum. The contribution of two-phonon states is plotted by a curve with triangles. The full curve is the total calculated cross section.

2.3 Anharmonicities

Another possible effect arises from a shift of the energy centroid of the DGDR due to anharmonic effects [23]. In ref. [22] one obtained $\sigma_{DGDR} = 620$, 299 and 199 mb for the centroid energies of $E_{DGDR} = 20$, 24 and 27 MeV, respectively. This shows that anharmonic effects can play a big role in the Coulomb excitation cross sections of the DGDR, depending on the size of the shift of E_{DGDR}. However, in ref. [20] the source for anharmonic effects were discussed and it was suggested that it should be very small, i.e., $\Delta^{(2)}E = E_{DGDR} - 2E_{GDR} \simeq 0$. The anharmonic behavior of the giant resonances as a possibility to explain the increase of the Coulomb excitation cross sections has been studied by several authors [23,24] (see also ref. [25], and references therein). It was found that the effect is indeed negligible and it could be estimated [25] as $\Delta^{(2)}E < E_{GDR}/(50A) \sim A^{-4/3}$ MeV. Recent studies [26] of the reaction mechanism with anharmonic effects support the idea that these are indeed very small.

2.4 Other routes to the DGDR

From the above discussion we see that the magnitude of the Coulomb excitation cross sections of the DGDR can be affected due to uncertainties in: (a) strength, (b) width, (c) energies, or (d) reaction mechanism. Cases (a) and (c) are the basis of the Axel-Brink hypothesis and we have seen that a modification of their values would only be considered seriously if anharmonic effects were large, which does not seem to be the case. Case (b) is an open question. Microscopic calculations [24] have shown that, taking into account the Landau damping, the collective state splits into a set of different 1^-_i states distributed over an energy interval, where i is the order number of each state. A further fragmentation of the 1^-_i states into thousands of closed packed states, is obtained by the coupling of one- and two-phonon states. This leads to a good estimate of the spreading width of the GDR. However, the DGDR states were obtained by a folding procedure:

$$|[1^-_i \otimes 1^-_{i'}]_{J^\pi=0^+,1^+,2^+} >_M = \sum_{m,m'} (1m1m'|JM)|1^-_i >_m |1^-_{i'} >_{m'} . \qquad (8)$$

The width of the DGDR is thus fixed by the width of the GDR. It is therefore impossible

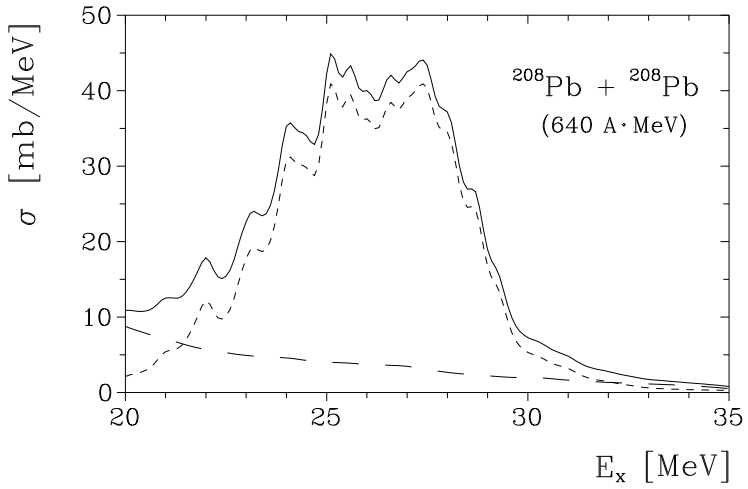

Figure 5: The contribution for the excitation of two-phonon 1^- states (long-broken curve) in first-order perturbation theory, and of two-phonon 0^+ and 2^+ DGDR states to second-order (short-broken curve). The total cross section (for ^{208}Pb(640.A MeV) + ^{208}Pb) is shown by the full curve.

to make any quantitative prediction for the width of the DGDR, other than saying that $\sqrt{2} \leq \Gamma_{DGDR}/\Gamma_{GDR} \leq 2$. Thus, we return to the discussion of the reaction mechanism, and how it could affect the magnitude of the cross sections. The nuclear excitation of giant resonances is very small in magnitude compared with Coulomb excitation in collisions with heavy ions at relativistic energies [22]. In ref. [22] it was shown that the nuclear-Coulomb interference is also a small effect.

In ref. [27] the contribution of non-natural parity 1^+ two-phonon states were investigated in a coupled-channels calculation. The diagonal components $[1_i^- \otimes 1_i^-]_{1^+}$ are forbidden by symmetry properties but non-diagonal ones $[1_i^- \otimes 1_{i'}^-]_{1^+}$, may be excited in the two-step process bringing some "extra strength" in the DGDR region. Consequently, the role of these non-diagonal components depends on how strong the Landau damping is. A coupled-channels calculation found that the contribution of the 1^+ states to the total cross section is small. The reason for this is better explained in second-order perturbation theory. For any route to a final magnetic substate M, the second-order amplitude will be proportional to $(001\mu|1\mu)V_{E1\mu,0\to 1^-} \times (1\mu 1\mu|1M)V_{E1\mu,1^-\to 1^+} + (\mu \leftrightarrow \mu')$, where $V_{E1\mu,i\to f}$ is the μ-component of the interaction potential (for a spin-zero ground state, μ is also the angular momentum projection of the intermediate state). Assuming that the phases and the products of the reduced matrix elements for the two sequential excitations are equal, we obtain $V_{E1\mu,0\to 1^-} \times V_{E1\mu',1^-\to 1^+} = V_{E1\mu',0\to 1^-} \times V_{E1\mu,1^-\to 1^+}$. Thus, under these circumstances, and since $(001\mu|1\mu) = 1$, we get an identically zero result for the excitation amplitude of the 1^+ DGDR state as a consequence of $(1\mu 1\mu|1M) = -(1\mu' 1\mu|1M)$.

We note that multiphonon states can be obtained by coupling all kinds of phonons. Each configuration $[\lambda_1^{\pi_1} \otimes \lambda_2^{\pi_2}]$ can be obtained theoretically from a sum over several two-phonon states made of phonons and of complicated states with a given spin and parity $\lambda_1^{\pi_1}$, $\lambda_2^{\pi_2}$, and different RPA root numbers i_1 , i_2 of their constituents. The cross sections can be obtained accordingly:

$$\sigma([\lambda_1^{\pi_1} \otimes \lambda_2^{\pi_2}]) = \sum_{i_1,i_2} \sigma([\lambda_1^{\pi_1}(i_1) \otimes \lambda_2^{\pi_2}(i_2)]). \tag{9}$$

As an example, in ref. [28] the total number of two-phonon 1^- states generated in this way was about 10^5. The absolute value of the photoexcitation of any two-phonon state under consideration is negligibly small but altogether they produce a sizeable cross section. The 1^- two-phonon states obtained in ref. [28] were used to calculate their contribution to the (γ,n) cross section

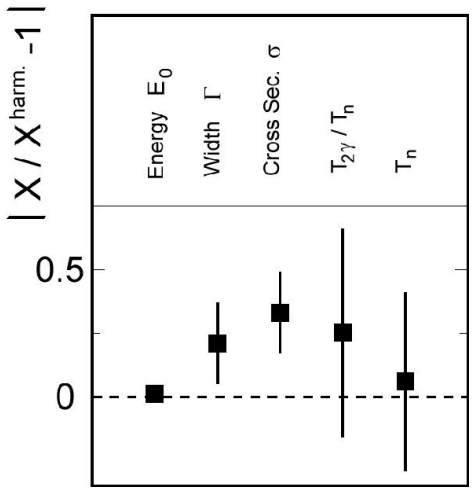

Figure 6: Deviation of the experimental results from the harmonic oscillator prediction for the energy, width, cross section, ratio between the decay by emission of two gammas, and of the one—neutron decay width, respectively.

in ^{208}Pb, via direct E1 excitations. This is shown in figure 4. Experimental data (dots with experimental errors) are from [29]. The long-broken curve is the high-energy tail of the GDR, the short-broken curve is the IVGQR and the curve with squares is their sum. The contribution of two-phonon 1^- states is plotted by a curve with triangles. The full curve is the total calculated cross section. Thus, already at the level of photonuclear data the contribution of two-phonon 1^- states is of relevance. Here they are not reached via two-step processes, but in direct excitations. Since the energy region of these states overlap with that of the DGDR, in Coulomb excitation experiments they should also contribute appreciably. In fact, it was shown [28] that their contribution to the total cross section for ^{208}Pb + ^{208}Pb (640.A MeV) in the DGDR region is of the order of 15%. In figure 5 we show the contribution of the excitation of two-phonon 1^- states (long-dashed curve) in first order perturbation theory, and for two-phonon 0^+ and 2^+ DGDR states in second-order (short-dashed curve). The total cross section (for ^{208}Pb (640.A MeV) + ^{208}Pb) is shown by the solid curve.

3 Present situation and perspectives

Presently, experiments tell us that the harmonic model reproduces the cross section for the GDR quite well, but it gives smaller values than the measured cross sections by as much as 30%. In figure 6 the present situation on our knowledge of the energy, width, excitation cross section, branching ratio for gamma to neutron emission, and the neutron emission width, respectively, is shown in comparison with calculations based on the simple harmonic picture. We see that the theory-experiment agreement is much better than that obtained in the pioneer experiments. As we have seen in this short review there are several effects which compete in the excitation of double giant resonances in relativistic Coulomb excitation. These effects were discovered in part by the motivation to explain discrepancies between the harmonic picture of the giant resonances and the recent experimental data. We cannot say at the moment how much we have progressed towards a better understanding of these nuclear structures, as some controversies still remain in the literature (see, for example, [30]). Recent studies of giant resonances in ultra-relativistic collisions have been performed at CERN [31] and Brookhaven [32]. Since the nuclei fragment after the excitation to a giant resonance, this process can be used for beam monitoring as well [32]. The field is just in its infancy and important experimental and theoretical progress will occur in the

near future.

References

1. W. Bothe and W. Gentner, Z. Phys. **106**, 236 (1937)
2. M. Goldhaber and E. Teller, Phys. Rev. **74**, 1046 (1948)
3. H. Steinwedel and J.H.D. Jensen, Z. Naturf. **5a**, 413 (1950)
4. J. Speth and J. Wambach, Int. Review of Nuclear and Particle Physics vol. 7, ed. J Speth (Singapore, World Scientific), 1991
5. C.A. Bertulani and V.P. Ponomarev, Phys. Rep. **321**, 139 (1999)
6. J. Barrette et. al., Phys. Lett. **B209**, 182 (1988)
7. J. Beene et. al., Phys. Rev. **C41**, 920 (1990)
8. J. Beene, Int. Nuclear Physics Conf. on Giant Resonances (Gull Lake, 1993) (1994 Nucl. Phys. **A569** 163c
9. G. Baur and C.A. Bertulani, Phys. Lett. **B174**, 23 (1986); Phys. Rev. **C34**, 1654 (1986)
10. C.A. Bertulani and G. Baur, Phys. Rep. **163**, 299 (1988)
11. C.A. Bertulani and A.M. Nathan, Nucl. Phys. **A554**, 158 (1993)
12. S. Mordechai et. al., Phys. Rev. Lett. **61**, 531 (1988)
13. R. Schmidt et. al., Phys. Rev. Lett. **70**, 1767 (1993)
14. J.L. Ritman et. al., Phys. Rev. Lett. **70**, 2659 (1993)
15. A.C. Vasconcellos–Gomes and C.A. Bertulani, Nucl. Phys. **A517**, 639 (1990)
16. T. Aumann et. al. Phys. Rev. **C47**, 1728 (1993)
17. K. Boretzky et. al., Phys. Lett. **B384**, 30 (1996)
18. Ph. Chomaz and N. Frascaria, Phys. Rep. **252**, 275 (1995)
19. G. Baur and C.A. Bertulani, Proc. Int. School of Heavy Ion Physics (Erice, Italy, October 1986), ed. R.A. Broglia and G.F. Bertsch (New York: Plenum), p. 331
20. C.A. Bertulani and V. Zelevinsky, Phys. Rev. Lett. **71**, 967 (1993); Nucl. Phys. **A568**, 931 (1993)
21. L.F. Canto, A. Romanelli, M.S. Hussein and A.F.R. de Toledo Piza, Phys. Rev. Lett. **72**, 2147 (1994)
22. C.A. Bertulani, L.F. Canto, M.S. Hussein and A.F.R. de Toledo Piza, Phys. Rev. **C53**, 334 (1996)
23. C. Volpe et. al., Nucl. Phys. **A589**, 521 (1995) E. Lanza et. al., Nucl. Phys. **A613**, 445 (1997)
24. V. Ponomarev et. al., Phys. Rev. Lett. **72**, 1168 (1994); Z. Phys. **A356**, 251 (1996)
25. G.F. Bertsch and H. Feldmeier, Phys. Rev. **C56**, 839 (1997)
26. D.T. de Paula, T. Aumann, L.F. Canto, B.V. Carlson, H. Emling and M.S. Hussein, Phys. Rev. **C64**, 064605 (2001); C.A. Bertulani, Comput. Phys. Commun. **116**, 345 (1999)
27. C.A. Bertulani, V. Ponomarev and V.V. Voronov, Phys. Lett. **B388**, 457 (1996)
28. V. Ponomarev and C.A. Bertulani, Phys. Rev. Lett. **79**, 3853 (1997)
29. S.N. Belyaev et. al., Phys. At. Nucl. **58**, 1833 (1995)
30. C.A. Bertulani, P.F. Bortignon, V.Yu. Ponomarev and V.V. Voronov, Phys. Rev. Lett. **87**, 269201 (2001)
31. S. Datz et. al., Phys. Rev. Lett. **79**, 3355 (1997)
32. S. White, private communication